

Adaptation to HIF1 α deletion in hypoxic cancer cells by upregulation of GLUT14 and creatine metabolism

Alessandro Valli^{1,2}, Matteo Morotti¹, Christos E. Zois¹, Patrick K. Albers³, Tomoyoshi Soga⁴, Katharina Feldinger¹, Roman Fischer², Martin Frejno², Alan McIntyre¹, Esther Bridges¹, Syed Haider¹, Francesca M. Buffa¹, Dilair Baban³, Miguel Rodriguez^{5,6}, Oscar Yanes^{5,6}, Hannah J. Whittington⁷, Hannah A. Lake⁷, Sevasti Zervou⁷, Craig A. Lygate⁷, Benedikt M. Kessler^{2,8}, and Adrian L. Harris^{1,8}

¹Weatherall Institute of Molecular Medicine, University of Oxford, Oxford UK; ²Target Discovery Institute, Nuffield Department of Medicine, University of Oxford, Oxford, UK; ³The Wellcome Trust Centre for Human Genetics, University of Oxford, Oxford UK; ⁴Institute for Advanced Biosciences, Keio University, Tsuruoka, Yamagata, Japan; ⁵Metabolomics Platform, IISPV, Department of Electronic Engineering, Universitat Rovira i Virgili, Tarragona, Spain ; ⁶Spanish Biomedical Research Center in Diabetes and Associated Metabolic Disorders-CIBERDEM, Madrid, Spain ; ⁷Division of Cardiovascular Medicine, Radcliffe Department of Medicine , University of Oxford, Oxford, UK; ⁸equal senior authors

Running title: Energy profiling in hypoxic cancer cells

Keywords: Cancer Metabolism, Creatine, Glucose Transporter 14, HIF1 α , Hypoxia

Corresponding author: Alessandro Valli, Molecular Oncology Laboratories, Oxford

25 University, Department of Oncology, Weatherall Institute of Molecular Medicine, John
26 Radcliffe Hospital Oxford OX3 9DS. Email: alevalli14@gmail.com
27
28 The authors declare no conflict of interest.
29
30 Word count (without Reference and Figure legends) 5031
31
32 Total number of figures 7

ABSTRACT (233 words)

Hypoxia-inducible factor 1 α is a key regulator of the hypoxia response in normal and cancer tissues. It is well recognised to regulate glycolysis and is a target for therapy. However, how tumour cells adapt to grow in the absence of HIF1 α is poorly understood and important to understand for developing targeted therapies and the flexibility of the metabolic response to hypoxia via alternative pathways. We analysed pathways that allow cells to survive hypoxic stress in the absence of HIF1 α , using the HCT116 colon cancer cell line with deleted HIF1 α versus control. Spheroids were used to provide a 3D model of metabolic gradients. We conducted a metabolomic, transcriptomic and proteomic analysis and integrated the results. These showed surprisingly that in three-dimensional growth a key regulatory step of glycolysis is Aldolase A rather than phosphofructokinase. Furthermore, glucose uptake could be maintained in hypoxia through upregulation of GLUT14, not previously recognised in this role. Finally, there was a marked adaptation and change of phosphocreatine energy pathways, which made the cells susceptible to inhibition of creatine metabolism in hypoxic conditions. Overall, our studies show a complex adaptation to hypoxia that can bypass HIF1 α , but is targetable and it provides new insight into the key metabolic pathways involved in cancer growth.

Implications: Under hypoxia and HIF1 blockade, cancer cells adapt their energy metabolism via upregulation of the GLUT14 glucose transporter and creatine metabolism providing new avenues for drug targeting.

INTRODUCTION

Highly proliferating cancer cells must increase the import of nutrients and adopt a metabolic program that fulfils energetic, redox, and biosynthetic requirements for increasing cell mass. Metabolic flexibility is acquired through genetic and non-genetic factors that allow tumors to grow in altered biochemical conditions such as hypoxia, acidic pH, and a nutrient-poor microenvironment (1).

Warburg described the increase of oxidation of glucose into lactate in cancer cells (2). Although yielding less ATP than OXPHOS, glycolysis is utilised predominantly by cancer cells and provides a more rapid response to the high energy demand of rapidly proliferating cancer cells (3). In hypoxia, this regulation represents the predominant way to produce ATP, even for normal cells (1). Although many solid tumours demonstrate the Warburg effect some, such as prostate cancer, do not (4). Virus-infected cells show increased glucose metabolism and CD4 + T cell growth is characterized by a high synthesis of ATP and biosynthetic reactions (cell membrane and DNA biosynthesis). These observations show that, uncoupling glycolysis from OXPHOS can offer a metabolic solution adequate beneficial for the high energy demand while maintaining redox balance and biosynthetic requirements (5-7). Similarly, reprogramming of cancer metabolism activates distinct pathways in which oncogenic mutations convey downstream signals to directed pro-metabolic traits (1).

Adaptation to the hypoxic tumor microenvironment is driven by hypoxia inducible factors HIF1 α and HIF2 α that induce a distinct transcriptional program (8). HIF1 α regulates numerous metabolic genes, especially those involved in glycolysis and related auxiliary processes (9).

Because of the importance of HIF1 in tumor growth and the potential of HIF1 α as target, we investigated how a cell line deleted for HIF1 α could survive in hypoxia. We studied the HCT116 colorectal cancer (CRC) cell line wildtype (WT) and HIF1 α knockout (KO) under

78 hypoxic conditions and analyzed transcriptomics, proteomics, metabolomics, and fluxomics.
79 We integrated the multi-omics data to construct a map of hypoxic CRC cell energy
80 metabolism. Our results show for the first time upregulation of glucose transporter type 14
81 (GTR14) to maximize nutrient uptake and an important role for creatine (Cr) energy
82 pathways to sustain multidimensional growth under hypoxic conditions.

MATERIALS AND METHODS

Cell culture

Cell lines were available from Clare Hall Laboratories (HCT116), or were a kind gift from Prof Walter Bodmer (Weatherall Institute of Molecular Medicine, Oxford, United Kingdom; DLD-1, Ls174T). Cell line authentication was carried out by STR analyzes (LGC Standards) 6 months prior to the first submission of the manuscript. Cell were cultured as described before, unless different conditions were specified (10).

Enzyme activity assay

WT and KO HCT116 cells were cultivated at either 21% O₂ or 1% O₂ for 24 hours. Cells were collected, pelleted and suspended in 1ml of ice buffer (0.08mM K₂HPO₄, 1mM EGTA, 0.02mM KH₂PO₄, and 1mM β-mercaptoethanol whilst under experimental conditions. Samples were vortexed and 150μl aliquots removed for determination of protein by the Lowry method. A final concentration of 0.1% v/v triton X-100 was added to permeabilize cells. Samples were stored on ice for at least 30 minutes to allow precipitation and the supernatant was used for all enzyme activity measurements.

Total creatine kinase activity

20μl of 1:5 (in ice buffer) diluted sample supernatant was incubated with 1ml of CK-NAC reagent (Thermo Fisher Scientific) at 30°C. After 3 minutes lag time, CK activity was quantified spectrophotometrically by measuring the increase in absorbance at 340nm over 2 minutes as a result of NADH production. The assay was performed in triplicate and results normalized to protein concentration .

Relative activity of creatine kinase isoenzymes

Sample supernatant was diluted 1:200 in ice buffer and incubated with 1% CK isoenzyme activator for 10 minutes prior to use. Creatine kinase isoenzymes were separated according to their electrophoretic mobility on an agarose gel, followed by incubation with CK isoenzyme chromogen which allowed visualization of the bands. Relative activities of individual CK isoenzymes were quantified by densitometry. All reagents were provided within the SAS-1 CK VIS-12 Isoenzyme kit, Helena Biosciences. Absolute activities for each isoenzyme were calculated by multiplying relative isoenzyme activity by total CK activity.

Citrate synthase activity

50µl of sample supernatant was incubated with 850µl of reaction mixture (0.35mM acetyl-CoA, 0.12mM DTNB) at 25°C. After 3 minutes, 100µl of 1mM oxaloacetate was added into the reaction mixture. CS activity was immediately assessed spectrophotometrically by measuring the increase in absorbance at 412nm over 1 minute as a result of 5-thio-2-nitrobenzoate (TNB²⁻) production. The assay was performed in duplicates and results were normalized by protein concentration.

RESULTS

HIF1 α regulates hypoxic spheroid cancer growth

We cultured WT and KO HCT116 cells as spheroids (WTs and KOs) for 72 hours (h), generating a hypoxic inner mass, and evaluated their morphology at three time points (72.5, 76, 96 h). Immunostaining of WTs and KOs spheroids at 96 h showed key differences in hypoxic adaptation. Pimonidazole (PIMO) positive staining, in both WTs and KOs, confirmed the presence of hypoxic areas, and carbonic anhydrase 9 (CA9) (HIF1 α -target) positive stain in WTs demonstrated the presence of hypoxia and HIF1 α stabilization. In contrast, CA9 staining was absent in KOs, demonstrating successful HIF1 α knockout. Necrosis and cell death, as measured by H/E staining, was more pronounced in WTs than in KOs (Figure 1A).

We evaluated differences in growth of WTs and KOs (Figure 1B). HCT116 WTs and KOs proliferated over 24h, with a higher rate in WTs (upper panel). WTs volume was overall significantly bigger than that of KOs cells with no marked changes over time (middle panel). Cell spheroid density (number of cells per spheroid/spheroid volume) showed a significant increased over time in both WTs and KOs and was more pronounced in KOs at 96 h (lower panel).

HIF1 α metabolic effects in cancer spheroids

Since WTs and KOs grow unequally we optimized the formation of WTs and KOs with a comparable cell number, morphology, volume, and diameter which enabled the investigation of hypoxic gradients at the studied time points (72.5, 76, 96 h) (Data not shown). We measured 26 metabolites of six metabolic pathways: glycogen (GLG), glycolysis (GLY), TCA cycle, ATP, Cr, and redox metabolism (Figure 1C). GLG metabolic intermediates show a general decrease over time in both WTs and KOs. Glycolysis and Cr metabolic products

accumulated mostly in WT. TCA cycle metabolites did not show a defined trend, but generally appeared to be more elevated in WT 96 h and decreased in KO over time. We observed higher amounts of ATP in WT vs KO, and this difference remained stable over time; ADP levels decreased at 96 h in both in WT and KO. NAD^+ levels were low overall, while ADP and AMP were lower in KO vs WT. HIF1 α deletion correlated with higher AMP compared to ATP, but with less difference over time (Figure 1D). S1 shows statistical results for the metabolites detected in WT and KO.

Glycolytic and TCA flux in spheroids in hypoxia without HIF1 α

We next evaluated glycolysis and TCA cycle flux in spheroids in the presence and absence of HIF1 α . Spheroids were grown for 72 h and we utilized $^{13}\text{C}_6$ Glucose (Glu) for metabolic flux analysis (MFA) (Figure 2A). We calculated the isotopologue ratio for each metabolite as [single fully labelled isotopologue value]/[sum of the total isotopologue value] ratio (STIR). Next, we evaluated glycolysis and TCA STIR distribution. We noted that the overall STIR range was wider for metabolites of glycolysis compared to the TCA cycle (STIR glycolysis 0.2 to 0.8; STIR TCA cycle: 0.3 to 0.45).

In glycolytic MFA (Figure 2B), Glu 6 phosphate (Glu-6P) STIR increased linearly in WT between 72.5-96 h, increased significantly in WT vs KO at 96 h, but remained stable in KO. No effect was observed on $^{13}\text{C}_6$ fructose 6 phosphate (Fru-6P) MFA. Fructose 1, 6 bis phosphate (Fru-1,6BP) STIR decreased linearly in WT between 72.5-96 h, but remained stable in KO. No effect was observed on $^{13}\text{C}_6$ dihydroxyacetone phosphate (DHAP), 3-phosphoglycerate (3-PG), 2-phosphoglycerate (2-PG), and phosphoenolpyruvate (PEP) MFA in either spheroid type. Pyruvate (Pyr) and lactate STIR levels increased in WT 96 h vs earlier time points, whereas they accumulated earlier and to higher levels (76 h) in KO.

In the TCA MFA (Figure 2C), citrate STIR showed a linear increase in KOs. It was significantly lower in KOs than in WTs at 72.5 h and became significantly higher at 96 h, whereas citrate STIR remained stable in WTs. These data matched citrate synthase activity and its allosteric enzymatic regulator $\text{NAD}^+/\text{NADH}+\text{H}^+$ ratio both of which showed a significant increase only in HCT116 KO hypoxic cells (KOH) (Figure 2D). Cis-aconitate, isocitrate, succinate STIR was essentially unchanged, but cis-aconitate accumulated in KOs at 96 h. Alpha-KG and fumarate STIR were not assessed as only the unlabeled isotopologues were detected. Malate STIR increased linearly in KOs between 72.5-96 h and was significantly higher than in WTs at 96 h. Malate STIR showed a mild increase between 72.5-96 h in WTs (Figure 2C). Thus, glucose uptake was maintained without HIF1 α and a clear block of conversion of Fru-1,6BP to DHAP occurred without HIF1 α , at aldolase level, rather than the earlier step of conversion by phosphofructokinase of Fru-6P to Fru-1,6BP. There was, in addition, a surprising higher lactate and Pyr without HIF1 α . Because of this unexpected effect in the aldolase step on the glycolytic flux, we evaluated the clinical relevance of aldolase in CRC. We investigated whether tumour ALDOA mRNA expression levels correlated with patient prognosis using overall survival data derived from a cohort of 440 colon adenocarcinoma patients (TGCA). We found that, when the patient group was divided in quartiles, the highest quartile had a reduced five-year survival -Kaplan-Meier analysis of overall survival, Log-Rank $p < 0.05$ (S2A).

HIF response in 2D growth

For further manipulations of the cells, we used 2D growth. We initially confirmed the biology for HCT116 WT and KO cells in normoxia (N) and hypoxia (H) (WTN, KON, WTH, and KOH) (10). Hypoxia reduced proliferation in WTH and KOH cells, and the lack

of HIF1 α reinforced this effect in both normoxia and hypoxia (Figure 3A). We observed no difference in cell proliferation when experiments were conducted in 5mM or 25 mM Glu (Data not shown). HIF1 α expression was barely detectable in WTN, strongly accumulated in WTH, and was absent in both KON and KOH. CA9 accumulated only in WTH. HIF2 α doubled in expression in both WTH and KOH vs WTN and KON, showing no notable compensatory effect in the absence of HIF1 α (Figure 3B). In the 2D experiments we detected 27 metabolites (Figure 3C, 4A), 86 proteins (Figure 3D, E, 4B, C), and 76 mRNAs (Figure 4D) involved in ATP metabolism and related metabolic pathways that involve GLG, GLY, TCA cycle, ATP, Cr, redox, and adenosyl metabolism. We observed the highest ATP level in WTN. Both hypoxia and lack of HIF1 α lowered ATP in a cumulative fashion. Intracellular ADP did not show any significant differences. There was a significant increase in AMP levels in hypoxia, with the effect reinforced by the lack of HIF1 α in KOH (Figure 4E).

Analysis of metabolome. More small molecules accumulated in WTH and in KOH than in WTN and KON. Metabolites increased in WTH vs WTN were GLG, Glu, Glu-6P, 2-PG, lactate, and NAD⁺. Fumarate and malate were significantly increased in WTN. Comparing WTH vs KOH cells, a set of metabolites increased in KOH (Glu-1P, UDP-Glu, Fru-1,6BP, lactate, succinate, fumarate, malate, AMP, Cr). We assessed intracellular levels of PCr and Cr and calculated PCr /Cr ratio. We observed a decrease in ratio in WTH vs KOH ($p<0.01$); in addition, in both WTH and KOH the ratios were decreased vs their parental normoxic cells WTN and KON ($p<0.001$) (S6 A, B). Lactate levels were significantly increased in WTH if compared to WTN and further increased in KOH when compared to WTH, matching to the 3D flux (Figure 4A and 2B). TCA metabolites were elevated in KOH demonstrated the predominant role of HIF1 α in redirecting metabolism away from TCA cycle in hypoxia (Figure 3C, 4A).

Analysis of proteome. Many previously described enzymes were increased in WTH versus WTN (e.g. PGM1, GLGB, GTR1, HEXK1, G6PI, PFKAM,). Comparing WTH vs KOH cells, enzymes were similarly elevated in the WTH, demonstrating the predominant role of HIF1 α (PGM1, GLGB, GTR1, G6PI, PFKAM).

In contrast, in KOH versus WTH, UGPase, GYS1, GTR3/GTR14 (proteomics did not differentiate between the two transporters), PFKAL, PFKAP, PDP1, PDPR, ACLY, IDH3G, ADT2, ATAD2, KCRB, BLVRB, and ADK were up regulated. TIGAR was upregulated (but decreased in WTH vs WTN) (Figure 3D, E, 4B, C).

Analysis of transcriptome. We next evaluated mRNA features associated with the targeted proteomics signature. In WTH vs WTN we observed an increase of *GLGB*, *GSK3B*, *GTR1*, *GTR3/ GTR14*, *HEXK1*, *PFKAL*, *ALDOA*, *PGK1*, *PGAM1*, *ACON*, and many others. *PYGB*, *PDRP*, *IDH3A*, and *AAPK1* were down regulated.

When we evaluated KOH vs WTH we observed *PYGB*, *UGPase*, *GTR3* and/or *GTR14*, *TIGAR*, *FUMH*, *ATPD*, *ATAD2*, *BLVRB*, and *AAPK1* upregulated. However most of the genes were lower *GTR1*, *PGM2*, *GLGB*, *GSK3B*, *GTR1*, *G6PI*, *PGK1*, *PGAM1*, *PKM*, *ACON*, *IDH3G*, *KCRU*, and *KAD4* (Figure 4D).

HIF1 α and hypoxia-dependent effects on transcription and protein levels

We correlated transcriptomics and proteomics by calculating for each feature log₂-fold changes (FC) for mRNA and proteins comparing the following models: KON-WTN (HIF1 α effect in normoxia), WTH-WTN (HIF1 α effect in hypoxia), KOH-KON (HIF1 α independent hypoxia effects) and KOH-WTH (HIF1 α effect in hypoxia, expected to be similar to WTH-WTN).

We applied linear regression analysis to correlate mRNAs log₂ FC and proteins log₂ FC for each model. The correlation of WTN-WTH was similar to KOH-WTH. In contrast, KOH vs

KON showed no significant correlation. Interestingly, there was strong evidence for a normoxic effect of HIF1 α as the slope for KON versus WTN was similar to that for KOH versus WTH (S3).

Significantly regulated genes at either RNA and protein level (63 for WTH-WTN and 56 for KOH-WTH) were compared to evaluate transcription and/or translation patterns of regulation under hypoxia.

They are shown (protein and mRNA) in a heat-map of log₂ FC. For many previously well characterized genes there was a close correlation of mRNA and protein, but in some proteins went up proportionally more (ACON, ATP5J, ATAD2, GTR14) suggesting a stronger post translational element. In others, mRNA increased without a change in protein (GSK3B and TIGAR). The most regulated features were selected based on residuals below and above -2 σ and 2 σ distribution for each experimental condition (Figure 4D, S3).

Protein kinase AMPK expression showed a significant increase only in WTH vs WTN (50%, $p < 0.01$). Interestingly, p-AMPK was strongly expressed in absence of HIF1 α in both KON and KOH. AMPK/p-AMPK (levels normalized by β -actin) ratio was positive for KON and KOH, (13 and 9, respectively) while it was negative for WTN and WTH (S6C).

HIF1 α /HIF2 α hypoxic interaction regulates GTR14 expression

Flux analysis highlighted that Glu uptake was maintained in the absence HIF1 α ; thus, we studied in more detail Glu transporters in hypoxia. PCR analysis showed GTR3 and GTR14 more highly expressed in the absence of HIF1 α in normoxia. Both genes were induced in WT cells in hypoxia, but more highly induced in the KO cells, KOH (Figure 5A and 5B). Similar results were observed for more severe hypoxia O₂ 0.1% (S4A and S5A) and in two other CRC cell lines DLD1 (S4B and S5B), and Ls174T (S4C and S5C).

Western blot analysis showed GTR3 induced mostly in KOH and slightly in WTH. GTR14 was suppressed by HIF1 α in both WTN and WTH vs KON and KOH. Hypoxia, in absence of HIF1 α , reinforced GTR14 expression protein as shown by KOH vs KON (Figure 5C and S4E).

We studied the effects of HIF1 α and HIF2 α on GTR14 modulation in hypoxia. We utilized HCT116 WT cells HIF1 α and HIF2 α single knock down and HCT116 KO HIF2 α knock down exposed to 1% O₂ (WT1KDH, WT2KDH, KO2KDH). CA9 suppression in KON, WT1KDH, KOH, and KO2KDH vs WTN and WTH, confirmed HIF1 α absence. HIF2 α suppression in WT2KDH and KO2KDH vs WTH, WTKD1H, and KOH, confirmed HIF2 α knock down (S4D, S5D). *GTR1* RNA expression increased only in WTH and WT2KDH i.e. in response to HIF1 α (S4D, S5D). In normoxia, *GTR3* was higher in KO cells and further increased in the KOH. In hypoxia the levels increased in WT cells to the same level as KON. However, HIF2 α KD had only a small effect on the expression level in either cell line, suggesting that in the WT cells it is mainly HIF1 α regulated and the adaptation in KO cells is through a different pathway. Yet in DLD1 cells, HIF2 is clearly the factor involved in *GTR3* regulation in hypoxia (S4B).

GTR14 was higher in KON than in WTN, and in WTH increased to a similar but lower level than KON. KOH increased further than KON. WTKD1H had higher levels than WTH. Knockdown of HIF2 in the KO cells substantially reduced the high *GTR14* levels. These data support the potential role of HIF2 α competing with HIF1, so that in absence of HIF1, a great effect of HIF2 α occurs in hypoxia. Similar results were shown for DLD1 cells (S4B), where HIF2 α antagonised HIF1 α and induction was greater with HIF1 α KD, and ablated with HIF2 α knockdown. In western blot analysis of GTR3 and GTR14 (S4E) KOH had the highest levels of GTR3 and 14, reduced by HIF2 α KD, but not by HIF1 α KD in WT cells, which had the lowest levels of both transporters. No effect on cell proliferation was observed

when GTR3 was knocked down. However, GTR14 knock down showed a significant decrease of cell proliferation (about 40% in WTN and KON $p<0.001$; 50% WTH and KOH $p<0.01$ and $p<0.05$) after 24h cultivation in any of the studied experimental conditions, showing an high dependency of HCT116 on this glucose transporter (S7A). FC in HCT116 cells proliferation comparing normoxia and hypoxia upon GTR14 silencing in HIF1 α -deficient and control, showed significant reduction in KOH/WTH (FC= 0.3 ± 0.06) as compared to KON/WTN (FC= 0.6 ± 0.08 , $p<0.01$); WTH/WTN (FC= 0.5 ± 0.06 , $p<0.01$); KOH/KON (FC= 0.6 ± 0.1 , $p<0.001$). Finally, there was a reduction in proliferation when HIF2 α was knocked down, that was greater in KOH HCT116 cells (about 50% in WTN, KON, and WTH $p<0.001$ to $p<0.01$: and 60% in KOH $p<0.01$) (S7A).

HIF1 α differentially regulates expression of creatine kinase isoenzymes

Metabolic analysis highlighted Cr metabolism as a mechanism that could compensate for loss of HIF1 α activity by promoting the reversible reaction $\text{PCr} + \text{ADP} = \text{Cr} + \text{ATP}$. By proteomics analysis, KCRB was upregulated in absence of HIF1 α in both normoxia and hypoxia. KCRU was downregulated in absence of HIF1 α in both normoxia and hypoxia (Figure 3E and 4C). The expression also correlated with the transcriptomics data (Figure 4D). This data was then validated by PCR (Figure 5A and B) and by western blot (Figure 5D). These data were confirmed in two additional CRC cell lines, DLD1, and Ls174T (S4B, C, S5 B, C). The cytosolic enzyme KCRB was upregulated in absence of HIF1 α and the mitochondrial enzyme KCRU was up regulated in presence of HIF1 α (Figure 5D). KCRB dimer isoenzyme (KCRBB) activity (measured in whole cell extract) matched protein and mRNA expression (Figure 5E).

In addition, we found (by PCR analysis) that hypoxia up regulated cell membrane Cr transporter *SLC6A8* equally in WTH and KOH vs normoxia (Figure 5A and B).

Interestingly, total KCR activity in HCT116 cells showed the same changes as KCRBB (S7C, 5E). We evaluated total KCR activity also in MCF7 breast cancer cells WT or KO. In normoxia total MCF7 KCR activity was increased in KON vs WTN, showing a similar effect to HCT116 normoxic experiments. Also, no difference was observed between KON and KOH. However, in contrast, in hypoxia MCF7 KCR activity increased to the same level as KOH. This could reflect the much lower basal activity observed in this cell line (10 times lower than HCT116) (S7B, C, D). Finally, in CODREAD CRC patients *KCRU* (*CKMT1A*, and *CKMT1B* mitochondrial genes coding for *KCRU*) correlated positively with hypoxia signatures (S2B).

Creatine metabolism is essential for hypoxic tumor growth in absence of HIF1 α

We tested the effect of Cr metabolism on growth by using cyclocreatine (cc) to inhibit Cr kinase enzyme activity and methionine (Met) deprivation, precursor in Cr biosynthesis through the reaction mediated by S-adenosyl-L-methionine/Guanidinoacetate N-methyltransferase. In HCT116, we observed that after cc addition there was an overall reduction in proliferation in WT and KO in both normoxia and hypoxia (Figure 6A). In normoxia, Met deprivation significantly reduced cell proliferation. In hypoxia, the effect was less pronounced for KO cells and was not significant for WT HCT116 cells (Figure 6B), showing compensation by a partially HIF dependent pathway in hypoxia. We confirmed these results in the clonogenic capability of HCT116 cells with and without cc. Interestingly, only KONcc and KOHcc showed a significant reduction in clone formation with KOHcc substantially lower than KONcc (Figure 6C). Finally, in spheroids, cc decreased the volume in KO-cc treated (day 10) as compared to KO controls (Figure 6D, E and F). KCRB knocked down in HCT116 showed a significant reduction of cell proliferation of more than 50% in all experimental conditions (WTN< KON< and WTH $p<0.00$; KOH $p<0.01$) (S7E). FC in

345 HCT116 cells proliferation comparing normoxia and hypoxia upon KCRB silencing in
346 HIF1 α -deficient and control, showed significant reduction in KOH/WTH (FC=0.2 \pm 0.05)
347 compared to KON/WTN (FC=0.5 \pm 0.05, p <0.001); WTH/WTN (FC=0.3 \pm 0.03, p <0.05);
348 KOH/KON (FC=0.4 \pm 0.05, p <0.001). All together these results confirm the results of
349 cyclocreatine experiments.

DISCUSSION

In this study, we show how hypoxic cancer cells can metabolically compensate for HIF1 α loss in hypoxia. In particular, we identified two main adaptive metabolic processes allowing cancer cells to support and meet their energetic and precursors needs for proliferation in hypoxia in the absence of HIF1 α (Figure 7 summary diagram).

Hypoxic HIF1 α deficient cancer cells maintain a significant proliferation and metabolic capability. Several HIF1 α -independent hypoxic responses have been reported to sustain tumor growth via NF- κ B or PHD1/EglN2 (11-13) and support tumor metabolism via fructose and lipid metabolic pathways (10, 14). As expected, in hypoxia HIF1 α promotes GTR1 expression and a dynamic induction of Glu-6P intracellular gradient increase. This regulation, HIF1 α /PI3K/Akt mediated, ensures glucose supply to high glycolytic proliferating cancer cells (15).

However, in the absence of HIF1 α , we found that low GTR1 coexisted with a sustained intracellular Glu-6P level in hypoxia. This metabolic phenotype was associated with an induction of GTR3 and GTR14 at mRNA and protein level. GTR3 and GTR14 share 95% nucleotide identity (16), and GTR14 was thought to be a GTR3 variant (17). Indeed, we found that GTR14 antibody detection yielded a signal for both GTR3 and GTR14 proteins, while mass spectrometry analysis did not result in a high enough sequence coverage to discriminate between the two glucose transporters.

Adaptation of cancer cells to local glucose and Cr concentrations occurs by specific regulation of Glu transporters expression, glycolytic enzymes, or ATP levels (18, 19). In our data, GTR3 regulation did not display typical HIF2 α dependency although expressed at higher basal levels in the KO cells, it was induced in WT by hypoxia to the same level, suggesting in this case another mechanism, e.g. Nf κ B, has replaced HIF1 α (20) while GTR14 upregulation was driven by HIF2 α in the absence of HIF1 α . However, in DLD1, GTR3 is

clearly a HIF2 target, showing the variation that can occur in this regulation. Because of the high affinity for Glu, GTR3 overexpression could provide growth advantages in tumors already at low Glu levels (18). Interestingly, a link between hypoxia, GTR3, and Glu uptake was suggested to be important for lipid biosynthesis in macrophages (21). In line with this, HIF2 α was reported to play a major role in lipid metabolism (22). GTR14 has been associated with low survival in human testis and in gastric adenocarcinoma patients (23). Alternative mechanisms by which GTR3 and GTR1 can be regulated include HIF2 α via Ptpmt1 and HIF1 α via IGF-1 respectively (24, 25). The reason that GTR14KD but not GT3KD affects HCT116 cell proliferation may be related to relative flux through the pathways if GTR14 was the major transporter, or because GTR14 is also a dehydroascorbate transporter (26), but these require future analysis.

HIF1 α in hypoxia enhances tumor glycolytic enzymes expression and glycolytic flux (27). In hypoxia in the absence of HIF1 α , we found an accumulation of most of the glycolytic intermediates which was accompanied by low glycolysis enzymatic levels and glycolytic flux.

Our results match previous data in HCT116 HIF1 β KD and hepatoma cancer cells where Glu uptake was maintained in either normoxia or hypoxia despite the down-regulation of many glycolytic genes (28) with a mechanism that involved autophagy. An increase of Glu-6P and Fru-1,6BP metabolic flux not only contributes to glycolytic ATP production, but can also provide precursors for auxiliary pathways such as, glycogen, PPP, and lipids (10, 14, 29, 30). In hypoxia, in the absence of HIF1 α , we found a blockage at the metabolic step mediated by fructose-bisphosphate aldolase (Aldolase A, ALDOA), catabolizing the cleavage of Fru-1,6BP to glyceraldehyde 3-phosphate and dihydroxyacetone phosphate. Previously it has been shown that PFKB3 was key in regulating glycolysis one step earlier, and has been the focus of several approaches to develop inhibitors (31). Our data highlights that ALDOA

should be considered as a target for therapy now. ALDOA was shown to stabilize HIF1 α via PDH in lung cancer and to promote cancer progression *in vivo* (32, 33). ALDO is activated via PI3K, which recruits ALDO from the cytoskeleton and redistributes it in the cytosol where can increase glycolysis (34). Finally, ALDOA was shown to be induced by hypoxia in CRC-derived cell lines and to be an independent prognostic factor for CRC (35).

In hypoxia in the presence of HIF1 α , we found that Pyr and lactate levels were lower compared to HIF1 α KO. This could be due to a faster metabolism of Pyr into lactate by LDHA and its subsequent removal through transporters (15). As LDHA and lactate transporters are HIF1 α targets, this flux can be reduced in hypoxic HIF1 α deficient cells, thus explaining the observed high intracellular levels found for Pyr and lactate.

We also found that in hypoxia, citrate levels are elevated and Pyr oxidation into the TCA is overall maintained in the absence of HIF1 α . Under hypoxic conditions, HIF1 α drives phosphorylation of PDK that inhibits PDH and shunts Pyr away from mitochondria to lactate, reducing the rate of oxidative decarboxylation and diminishing acetyl-CoA formation (36). Consequently, replenishment of TCA cycle in mitochondria is altered. In such conditions, citrate biosynthesis is prevented, reductive carboxylation is enhanced, and a HIF1 α -dependent mechanism allows hypoxic cells to metabolize glutamine into fatty acids through citrate formation (37). Consistent with this, the high fully labelled malate content could be due to malate formation associated with a decreased malate transport outside the mitochondria (M2OM) and a reduced metabolism that is MDHM/MDHC-dependent (Figure 4). Finally, STIR reduction in TCA vs glycolysis (more evident in the presence of HIF1 α) shows the metabolic uncoupling that is HIF1 α -dependent in hypoxic cancer cells. Our finding that, in hypoxia, fully labelled citrate formation is favored and malate is accumulated in the absence of HIF1 α , suggests diminished reductive carboxylation as the predominant metabolic regulation.

In HCT116 spheroids and 2D hypoxic cells we found a strong increase of AMP levels in absence of HIF1 α . This was accompanied by a strong expression of p-AMPK in HCT116 KO cells only. Previous data report AMPK being activated in low-oxygen conditions by a HIF1 α -independent mechanism (38), potentially responding to cellular energy status through AMP binding to AMPK γ subunit, so promoting phosphorylation by upstream kinases and finally inhibiting AMPK dephosphorylation (39). In addition, in our results intracellular ATP levels were higher in the presence of HIF1 α , although ATP is maintained in its absence. This was found to be consistent with a generally reduced protein synthesis (as assessed by mRNA/protein ratios) as this process is a primary energy-consuming process can account for up to 70% of cellular ATP utilization (40). Under hypoxia, a rapid inhibition of global mRNA translation represents a major protective strategy to maintain energy (41).

However, ATP maintenance is a process linked to ATP re/generating metabolic systems that relies on biochemical regulatory systems at subcellular level (42). For example, in skeletal muscle, the high availability of PCr and Cr allows ATP maintenance by promoting the reversible reaction $\text{PCr} + \text{ADP} = \text{Cr} + \text{ATP}$. The Cr kinase system, highly expressed in human tissues with high-energy demand, can enhance neuromuscular performance on an anaerobic short extent and during anaerobic intermittent exercise (43). Indeed, active skeletal muscles capable of ATP anaerobic biosynthesis, keep global ATP reasonably constant during exercise.

This is accomplished by the Cr kinase metabolic system which replenishes the rate of ATP use at a fast pace (44). HIF2 α -modulated hypoxic response elements has been reported to be involved in Cr metabolism (45). Interestingly, our study shows that both in normoxia and hypoxia, HIF1 α maintains levels of the mitochondrial creatine kinase isoenzyme, KCRU, which was associated with a reduced TCA cycle. In contrast, the cytoplasmic creatine kinase isoenzyme, KCRB, is lower in WT cells. Strikingly, in cells without HIF1 α this distribution

was reversed, irrespective of hypoxia. This shows the importance of low levels of HIF1 α expression in regulating metabolic pathways. The complex effects of altering these enzymes on cell survival is shown by KCRU overexpression which enhanced the survival of breast cancer cells, while KCRB KD induced cell death in hypoxic ovarian cancer cells (43). Cr metabolism, which translocates ATP from sites of production to locations of ATP consumption, acts as a spatial/temporal energy buffer utilizing Cr, ATP, and ADP at distinct subcellular compartments (46). Consistent with this, colon cancer cells were shown to secrete KCRB extracellularly to generate and import PCr to enhance energy (19). *KCRB* and *KCRM* genes emerged as HIF2 α selective targets, and regulation of Cr kinase by HIF was shown in the gut (46), suggesting a role for HIF2 α in energy maintenance. In the absence of HIF1 α , we found that cc reduces HCT116 cell clonogenic capability and spheroid volume. KCRB depletion/inhibition in combination with chemotherapeutic agents showed synergistic effects in cancer therapy (47). Cr kinase metabolic inhibition by cc was shown to decrease cell viability, promote cell cycle arrest and apoptosis in EVI1 (48). Inhibition of the colon cancer cell line KCRB by pre-incubation with cc reduced liver metastasis formation and deplete PCr (49) and recently, mice inoculated with CRC cells and treated with cc showed a significant reduction in metastatic colonization (19). Our novel experimental work has shown that silencing of GTR14 or KCRB reduces the proliferation rate of HIF1 α -KO HCT116 cells in normoxic and hypoxic conditions. Since GRT14 and KCRB are more highly expressed in HIF1 α -KO hypoxic HCT116 cells, silencing these genes alters in a larger extent HCT116 HIF1 α -KO cells proliferation in hypoxia than control.

In summary, our work shows for the first time that hypoxic cancer cells harbor the capability to compensate for HIF1 α -deficient metabolic impasses by inducing GTR14 mediated Glu internalization in a HIF1 α /HIF2 α antagonistic fashion. We also report, Cr metabolism is tuned to function as a fast ATP buffering biochemical system. Aldolase A is shown to be a

control point in glycolysis by HIF1 α . As these alternate metabolic pathways were shown for the first time in 3D cancer cell cultures, they provide a model relevant to micrometastasis and drug targeting. Under hypoxia and HIF1 blockade, cancer cells adapt their energy metabolism via upregulation of the GLUT14 glucose transporter and creatine metabolism providing new avenues for drug targeting.

ACKNOWLEDGEMENTS

Financial support: this work was supported by a Cancer Research UK (CRUK) program grant (C602/A18974) to A.L.H; B.M.K. is supported by the Biomedical Research Centre (NIHR) Oxford, U.K; C.A.L is supported by British Heart Foundation Programme Grant (RG/13/8/30266).

References

1. Vander Heiden MG, Cantley LC, Thompson CB. Understanding the Warburg effect: the metabolic requirements of cell proliferation. *Science*. 2009;324(5930):1029-33.
2. Warburg O, Wind F, Negelein E. The Metabolism of Tumors in the Body. *J Gen Physiol*. 1927;8(6):519-30.
3. Pfeiffer T, Schuster S, Bonhoeffer S. Cooperation and competition in the evolution of ATP-producing pathways. *Science*. 2001;292(5516):504-7.
4. Eidelman E, Twum-Ampofo J, Ansari J, Siddiqui MM. The Metabolic Phenotype of Prostate Cancer. *Front Oncol*. 2017;7:131.
5. Palmer CS, Cherry CL, Sada-Ovalle I, Singh A, Crowe SM. Glucose Metabolism in T Cells and Monocytes: New Perspectives in HIV Pathogenesis. *EBioMedicine*. 2016;6:31-41.
6. Pavlova NN, Thompson CB. The Emerging Hallmarks of Cancer Metabolism. *Cell Metab*. 2016;23(1):27-47.
7. Liberti MV, Locasale JW. The Warburg Effect: How Does it Benefit Cancer Cells? *Trends Biochem Sci*. 2016;41(3):211-8.
8. Xie H, Simon MC. Oxygen availability and metabolic reprogramming in cancer. *J Biol Chem*. 2017;292(41):16825-32.
9. Mole DR, Blancher C, Copley RR, Pollard PJ, Gleadow JM, Ragoussis J, et al. Genome-wide association of hypoxia-inducible factor (HIF)-1alpha and HIF-2alpha DNA binding with expression profiling of hypoxia-inducible transcripts. *J Biol Chem*. 2009;284(25):16767-75.
10. Valli A, Rodriguez M, Moutsianas L, Fischer R, Fedele V, Huang HL, et al. Hypoxia induces a lipogenic cancer cell phenotype via HIF1alpha-dependent and -independent pathways. *Oncotarget*. 2015;6(4):1920-41.

- 527 11. Klein O, Rohwer N, de Molina KF, Mergler S, Wessendorf P, Herrmann M, et al. Application
 528 of two-dimensional gel-based mass spectrometry to functionally dissect resistance to targeted cancer
 529 therapy. *Proteomics Clin Appl.* 2013;7(11-12):813-24.
- 530 12. Rohwer N, Bindel F, Grimm C, Lin SJ, Wappler J, Klinger B, et al. Annexin A1 sustains
 531 tumor metabolism and cellular proliferation upon stable loss of HIF1A. *Oncotarget.* 2016;7(6):6693-
 532 710.
- 533 13. Li Y, Padmanabha D, Gentile LB, Dumur CI, Beckstead RB, Baker KD. HIF- and non-HIF-
 534 regulated hypoxic responses require the estrogen-related receptor in *Drosophila melanogaster*. *PLoS*
 535 *Genet.* 2013;9(1):e1003230.
- 536 14. Armitage EG, Kotze HL, Allwood JW, Dunn WB, Goodacre R, Williams KJ. Metabolic
 537 profiling reveals potential metabolic markers associated with Hypoxia Inducible Factor-mediated
 538 signalling in hypoxic cancer cells. *Sci Rep.* 2015;5:15649.
- 539 15. Schulze A, Harris AL. How cancer metabolism is tuned for proliferation and vulnerable to
 540 disruption. *Nature.* 2012;491(7424):364-73.
- 541 16. Augustin R. The protein family of glucose transport facilitators: It's not only about glucose
 542 after all. *IUBMB life.* 2010;62(5):315-33.
- 543 17. Schlosser HA, Drebber U, Urbanski A, Haase S, Baltin C, Berth F, et al. Glucose
 544 transporters 1, 3, 6, and 10 are expressed in gastric cancer and glucose transporter 3 is associated
 545 with UICC stage and survival. *Gastric Cancer.* 2015.
- 546 18. Birsoy K, Possemato R, Lorbeer FK, Bayraktar EC, Thiru P, Yucel B, et al. Metabolic
 547 determinants of cancer cell sensitivity to glucose limitation and biguanides. *Nature.*
 548 2014;508(7494):108-12.
- 549 19. Loo JM, Scherl A, Nguyen A, Man FY, Weinberg E, Zeng Z, et al. Extracellular metabolic
 550 energetics can promote cancer progression. *Cell.* 2015;160(3):393-406.
- 551 20. Christensen DR, Calder PC, Houghton FD. GLUT3 and PKM2 regulate OCT4 expression
 552 and support the hypoxic culture of human embryonic stem cells. *Scientific reports.* 2015;5:17500.

21. Li L, Liu B, Haversen L, Lu E, Magnusson LU, Stahlman M, et al. The importance of GLUT3 for de novo lipogenesis in hypoxia-induced lipid loading of human macrophages. *PloS one*. 2012;7(8):e42360.
22. Rankin EB, Rha J, Selak MA, Unger TL, Keith B, Liu Q, et al. Hypoxia-inducible factor 2 regulates hepatic lipid metabolism. *Mol Cell Biol*. 2009;29(16):4527-38.
23. Berlth F, Monig S, Pinther B, Grimminger P, Maus M, Schlosser H, et al. Both GLUT-1 and GLUT-14 are Independent Prognostic Factors in Gastric Adenocarcinoma. *Ann Surg Oncol*. 2015;22 Suppl 3:S822-31.
24. Xu QQ, Xiao FJ, Sun HY, Shi XF, Wang H, Yang YF, et al. Ptpmt1 induced by HIF-2alpha regulates the proliferation and glucose metabolism in erythroleukemia cells. *Biochemical and biophysical research communications*. 2016;471(4):459-65.
25. Yu J, Li J, Zhang S, Xu X, Zheng M, Jiang G, et al. IGF-1 induces hypoxia-inducible factor 1alpha-mediated GLUT3 expression through PI3K/Akt/mTOR dependent pathways in PC12 cells. *Brain research*. 2012;1430:18-24.
26. Amir Shaghaghi M, Zhouyao H, Tu H, El-Gabalawy H, Crow GH, Levine M, et al. The SLC2A14 gene, encoding the novel glucose/dehydroascorbate transporter GLUT14, is associated with inflammatory bowel disease. *Am J Clin Nutr*. 2017;106(6):1508-13.
27. Marin-Hernandez A, Gallardo-Perez JC, Ralph SJ, Rodriguez-Enriquez S, Moreno-Sanchez R. HIF-1alpha modulates energy metabolism in cancer cells by inducing over-expression of specific glycolytic isoforms. *Mini reviews in medicinal chemistry*. 2009;9(9):1084-101.
28. Frezza C, Zheng L, Tennant DA, Papkovsky DB, Hedley BA, Kalna G, et al. Metabolic profiling of hypoxic cells revealed a catabolic signature required for cell survival. *PLoS One*. 2011;6(9):e24411.
29. Favaro E, Bensaad K, Chong MG, Tennant DA, Ferguson DJ, Snell C, et al. Glucose utilization via glycogen phosphorylase sustains proliferation and prevents premature senescence in cancer cells. *Cell Metab*. 2012;16(6):751-64.

- 579 30. Bensaad K, Favaro E, Lewis CA, Peck B, Lord S, Collins JM, et al. Fatty acid uptake and
 580 lipid storage induced by HIF-1alpha contribute to cell growth and survival after hypoxia-
 581 reoxygenation. *Cell Rep.* 2014;9(1):349-65.
- 582 31. Lu L, Chen Y, Zhu Y. The molecular basis of targeting PFKFB3 as a therapeutic strategy
 583 against cancer. *Oncotarget.* 2017;8(37):62793-802.
- 584 32. Chang YC, Chan YC, Chang WM, Lin YF, Yang CJ, Su CY, et al. Feedback regulation of
 585 ALDOA activates the HIF-1alpha/MMP9 axis to promote lung cancer progression. *Cancer Lett.*
 586 2017;403:28-36.
- 587 33. Sanzey M, Abdul Rahim SA, Oudin A, Dirkse A, Kaoma T, Vallar L, et al. Comprehensive
 588 analysis of glycolytic enzymes as therapeutic targets in the treatment of glioblastoma. *PLoS One.*
 589 2015;10(5):e0123544.
- 590 34. Hu H, Juvekar A, Lyssiotis CA, Lien EC, Albeck JG, Oh D, et al. Phosphoinositide 3-Kinase
 591 Regulates Glycolysis through Mobilization of Aldolase from the Actin Cytoskeleton. *Cell.*
 592 2016;164(3):433-46.
- 593 35. Kawai K, Uemura M, Munakata K, Takahashi H, Haraguchi N, Nishimura J, et al. Fructose-
 594 bisphosphate aldolase A is a key regulator of hypoxic adaptation in colorectal cancer cells and
 595 involved in treatment resistance and poor prognosis. *Int J Oncol.* 2017;50(2):525-34.
- 596 36. Kim JW, Tchernyshyov I, Semenza GL, Dang CV. HIF-1-mediated expression of pyruvate
 597 dehydrogenase kinase: a metabolic switch required for cellular adaptation to hypoxia. *Cell Metab.*
 598 2006;3(3):177-85.
- 599 37. Metallo CM, Gameiro PA, Bell EL, Mattaini KR, Yang J, Hiller K, et al. Reductive glutamine
 600 metabolism by IDH1 mediates lipogenesis under hypoxia. *Nature.* 2011;481(7381):380-4.
- 601 38. Laderoute KR, Amin K, Calaoagan JM, Knapp M, Le T, Orduna J, et al. 5'-AMP-activated
 602 protein kinase (AMPK) is induced by low-oxygen and glucose deprivation conditions found in solid-
 603 tumor microenvironments. *Mol Cell Biol.* 2006;26(14):5336-47.
- 604 39. Li YH, Luo J, Mosley YY, Hedrick VE, Paul LN, Chang J, et al. AMP-Activated Protein
 605 Kinase Directly Phosphorylates and Destabilizes Hedgehog Pathway Transcription Factor GLI1 in
 606 Medulloblastoma. *Cell Rep.* 2015;12(4):599-609.

40. Koritzinsky M, Wouters BG. Hypoxia and regulation of messenger RNA translation. *Methods Enzymol.* 2007;435:247-73.
41. Staudacher JJ, Naarmann-de Vries IS, Ujvari SJ, Klinger B, Kasim M, Benko E, et al. Hypoxia-induced gene expression results from selective mRNA partitioning to the endoplasmic reticulum. *Nucleic Acids Res.* 2015;43(6):3219-36.
42. Kazak L, Chouchani ET, Jedrychowski MP, Erickson BK, Shinoda K, Cohen P, et al. A creatine-driven substrate cycle enhances energy expenditure and thermogenesis in beige fat. *Cell.* 2015;163(3):643-55.
43. Yan YB. Creatine kinase in cell cycle regulation and cancer. *Amino acids.* 2016;48(8):1775-84.
44. Khan JR, Iftikar FI, Herbert NA, Gnaiger E, Hickey AJ. Thermal plasticity of skeletal muscle mitochondrial activity and whole animal respiration in a common intertidal triplefin fish, *Forsterygion lapillum* (Family: Tripterygiidae). *J Comp Physiol B.* 2014;184(8):991-1001.
45. Zheng L, Kelly CJ, Colgan SP. Physiologic hypoxia and oxygen homeostasis in the healthy intestine. A Review in the Theme: Cellular Responses to Hypoxia. *Am J Physiol Cell Physiol.* 2015;309(6):C350-60.
46. Kitzenberg D, Colgan SP, Glover LE. Creatine kinase in ischemic and inflammatory disorders. *Clin Transl Med.* 2016;5(1):31.
47. Li XH, Chen XJ, Ou WB, Zhang Q, Lv ZR, Zhan Y, et al. Knockdown of creatine kinase B inhibits ovarian cancer progression by decreasing glycolysis. *Int J Biochem Cell Biol.* 2013;45(5):979-86.
48. Fenouille N, Bassil CF, Ben-Sahra I, Benajiba L, Alexe G, Ramos A, et al. The creatine kinase pathway is a metabolic vulnerability in EVI1-positive acute myeloid leukemia. *Nature medicine.* 2017;23(3):301-13.
49. Lillie JW, O'Keefe M, Valinski H, Hamlin HA, Jr., Varban ML, Kaddurah-Daouk R. Cyclocreatine (1-carboxymethyl-2-iminoimidazolidine) inhibits growth of a broad spectrum of cancer cells derived from solid tumors. *Cancer Res.* 1993;53(13):3172-8.

Figure 1. Spheroid hypoxic phenotype and energy metabolism

(A) Immunostaining of spheroids for protein expression of hypoxic markers. PIMO, CA9, and H/E expression in spheroid formed with HCT116 colorectal cancer cells HIF1 α (WT) and HIF1 α -deficient (KO).

(B) HIF1 α WT and KO spheroid morphology. Spheroid forming cell count (cell number, upper panel), spheroid volume (cm³, middle panel), and spheroid cell density (cell number/spheroid volume ratio, lower panel).

(C) Heatmap showing z normalized intensities of energy related metabolites in WT and KO spheroids at time points 72.5, 76, and 96 hours after formation. Relative Intensity (R.I).

(D) Specific ATP, ADP, AMP, ATP/AMP ratio, and ATP/ADP ratio relative intensities (R.I. 0-1 normalized) in WT and KO spheroids at time points 72.5, 76, and 96 hours after formation.

Metabolic pathways: glycogen (GLG), glycolysis (GLY), Krebs cycle (TCA), adenosine triphosphate (ATP), creatine (Cr), and oxidation-reduction (REDOX).

Data are reported as averaged \pm SD (N=3). Statistical comparisons were performed using two-way ANOVA, multiple post-hoc group comparisons, or t-test (p-values corrected for multiple testing using the Benjamini-Hochberg procedure at α =1%), showing p-value < 0.05 (*), < 0.01 (**), and < 0.001 (***).

Figure 2. Metabolic flux in spheroids

(A) Experimental design of metabolomics flux analysis in spheroids. (B and C) Glycolytic and TCA metabolic flux analysis after administration of $^{13}\text{C}_6$ glucose. Isotopologue quantification is shown by STIR ratio [single fully labeled isotopologue value]/[sum of the total isotopologue value].

(D) $\text{NAD}^+/\text{NADH}+\text{H}^+$ ratio and citrate synthase activity, WTN, KON, WTH, and KOH cells after 24 hours O_2 21% and 1%. Data are reported as averaged $\pm\text{SD}$ (N=3). Statistical comparisons were performed using two-way ANOVA, multiple post hoc group comparisons, or t-test (p-values corrected using the Benjamini-Hochberg procedure at $\alpha=1\%$), showing p-value < 0.05 (*), < 0.01 (**), and < 0.001 (***)).

Figure 3. Proteo-metabolomics profile of hypoxic HCT116

(A) WTN, KON, WTH, and KOH cell proliferation after 24 hours in two O₂ conditions, 21% and 1%. (B) Western blot analysis showing HIF1 α stabilization in hypoxia and successful deletion in KO HCT116 cells. HIF1 α , HIF2 α , and CA9 protein expression in cells: HIF1 α wild type normoxia (WTN), HIF1 α deficient normoxia (KON), HIF1 α wild type hypoxia (WTH), and HIF1 α deficient hypoxia (KOH). (C, D, E) Proteo-metabolomics heatmaps (C metabolites; D and E proteins) of the detected metabolites and proteins in WTN, KON, WTH, and KOH cells after 24 hours O₂ 21% and 1%. Normalized levels refer to WTN. Relative Intensity (R.I). Metabolic pathways: glycogen (GLG), glycolysis (GLY), Krebs cycle (TCA), adenosine triphosphate (ATP), creatine (Cr), oxidation-reduction (REDOX), and adenosyl metabolism. Data are reported as averaged \pm SD (N=3). Statistical comparisons were performed using two-way ANOVA, multiple post hoc group comparisons, or t-test, showing p-value < 0.05 (*), < 0.01 (**), and < 0.001 (***).

Figure 4. Analysis of HCT116 hypoxic metabolic phenotype

(A, B, C) Metabolomics and proteomics integrated circos-plots showing significantly regulated features only in KON vs WTN, WTH vs WTN, KOH vs KON, and KOH vs WTH (upper side circos-plots). Adjusted $p < 0.05$ (*) or $p < 0.01$ (**) are indicated for the different experimental comparisons (connecting lines inside circos-plots): KON/WTN (grey/white-grey connection) WTH/WTN (gold/white-brown connection), KOH/KON (blue/grey-violet connection), KOH/WTH (blue/gold-green connection). Coloured boxes (lower side circos-plots linked to connecting lines) represent different metabolic pathways, while coloured boxes (inside circos-plots linked to connecting lines) identify the biological condition where the feature is up-regulated. (D) Heatmap of integrated transomics (proteomics and transcriptomics); mRNA and proteins \log_2 fold change (FC) are calculated for WTH-WTN and KOH-WTH. Feature selection was based on departure from 95% confidence intervals of the linear model distribution built for each comparison (WTH-WTN and KOH-WTH). Metabolic pathways: glycogen (GLG), glycolysis (GLY), Krebs cycle (TCA), adenosine triphosphate (ATP), creatine (Cr), oxidation-reduction (REDOX), and adenosyl metabolism (ADE). (E) Targeted metabolomics showing distribution of ATP, ADP, AMP, ATP/AMP and ATP/ADP ratios in WTN, KON, WTH, and KOH cell after 24 hours in 21% and 1% O_2 . Raw intensities and ratios are shown as 0-1 normalized levels relative Intensity (R.I). Data are reported as averaged \pm SD (N=3). Statistical comparisons were performed using two-way ANOVA, multiple post hoc group comparisons, or t-test (p-values corrected using the Benjamini-Hochberg procedure at $\alpha=1\%$), showing p-value < 0.05 (*), < 0.01 (**), and < 0.001 (***).

Figure 5. Congruence between multi-omics metabolic reconstruction and hypoxia biochemistry

(A) PCR analysis of CA9, GTR1, GTR3, GTR14, HEXK1, KCRU, KCRM, and SLC6A8 mRNA levels in WTN, KON, WTH, and KOH cells after 24 hours O₂ 21% and 1%. (B) Statistical significance for PCR analysis measured features. (C and D) Western blot analysis of GTR14, GTR3, KCRB, KCRU, and KCRM in WTN, KON, WTH, and KOH cells after 24 hours O₂ 21% and 1%, and in WTs and KOs spheroids (96 hours). (E) Creatine kinase BB activity, WTN, KON, WTH, and KOH cells after 24 hours O₂ 21% and 1%.

Data are reported as averaged \pm SD (N=3). Statistical comparisons were performed using two-way ANOVA, multiple post hoc group comparisons, or t-test (p-values corrected using the Benjamini-Hochberg procedure at $\alpha=1\%$), showing p-value < 0.05 (*), < 0.01 (**), and < 0.001 (***).

Figure 6. Creatine metabolism is essential for hypoxic tumor growth in absence of HIF1 α

(A) Effect of cyclocreatine (cc) add on WTN, KON, WTH, and KOH cells after 24 hours O₂ 21% and 1%. (B) Effect of methionine deprivation on WTN, KON, WTH, and KOH cells after 24 hours O₂ 21% and 1%. (C and D) Effect of cyclocreatine (cc) add on WTN, KON, WTH, and KOH cell clonogenic (number of clones counted) after 24 hours O₂ 21% and 1%. (E and F) Effect of cyclocreatine (cc) add on HCT116 WT and KO spheroid growth (volume) at day 5, 8, and 10 (cc added after 3 after spheroid formation). Data are reported as averaged \pm SD (N=3). Statistical comparisons were performed using two-way ANOVA, multiple post hoc group comparisons, or t-test (p-values corrected using the Benjamini-Hochberg procedure at $\alpha=1\%$), showing p-value < 0.05 (*), < 0.01 (**), and < 0.001 (***)

Figure 7. The metabolic pathways and metabolites studied.

(A) Adaptation of hypoxic cancer cell metabolism by HIF1 α maintains energetic, redox, and biosynthetic requirements. (B) In this manuscript Valli *et al.* reveal for the first time that cancer cell growth and energy metabolism is maintained by HIF1 α -independent metabolic pathways under hypoxia which involve glucose uptake by GLUT14 and creatine metabolism. Metabolic pathways: glycogen (GLG), glycolysis (GLY), Krebs cycle (TCA), adenosine triphosphate (ATP), creatine (Cr), oxidation-reduction (REDOX), and adenosyl metabolism. (\uparrow) increase, (\downarrow) decrease, box size and lines/arrows thickness describe the regulation in the different conditions.

Figure 1

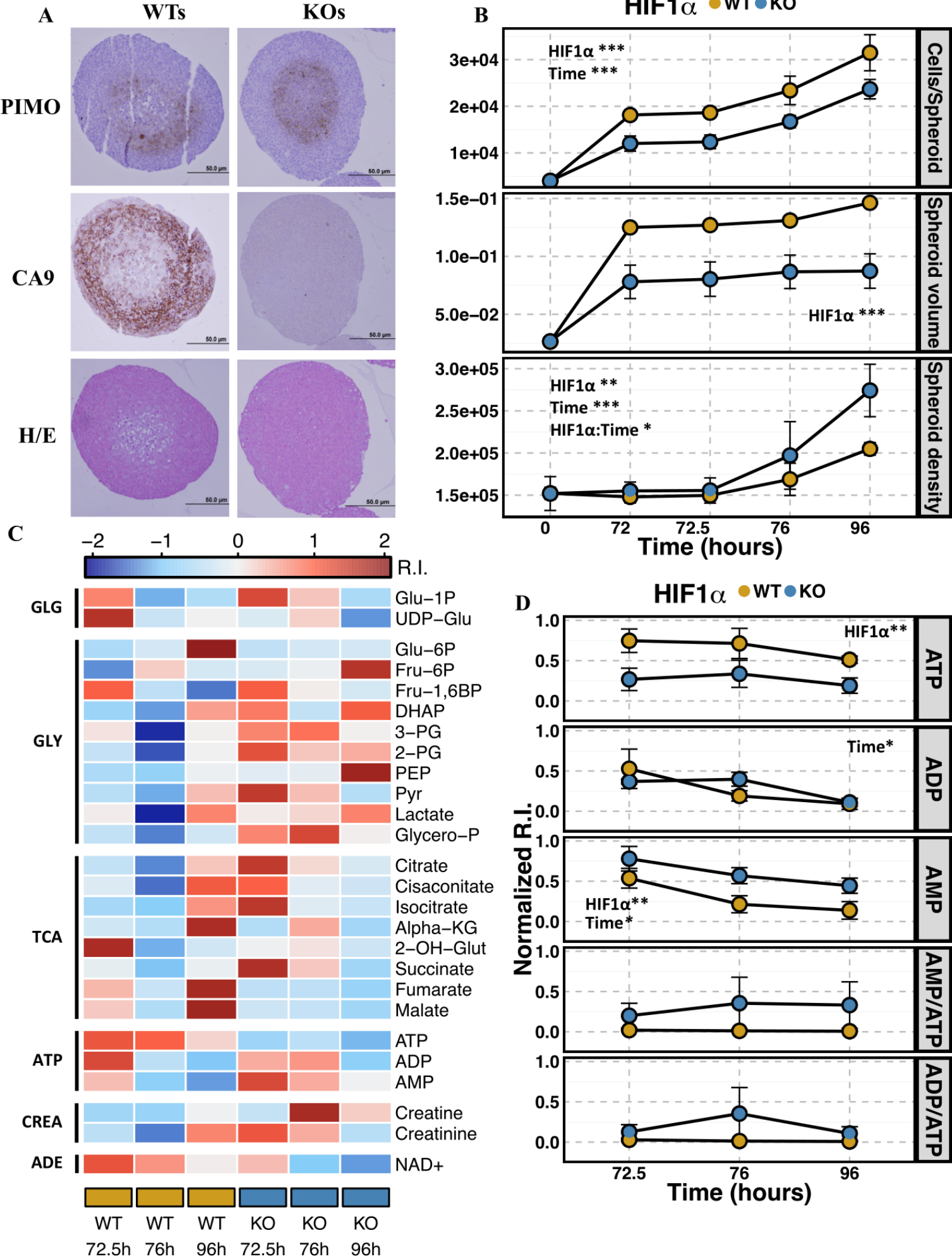
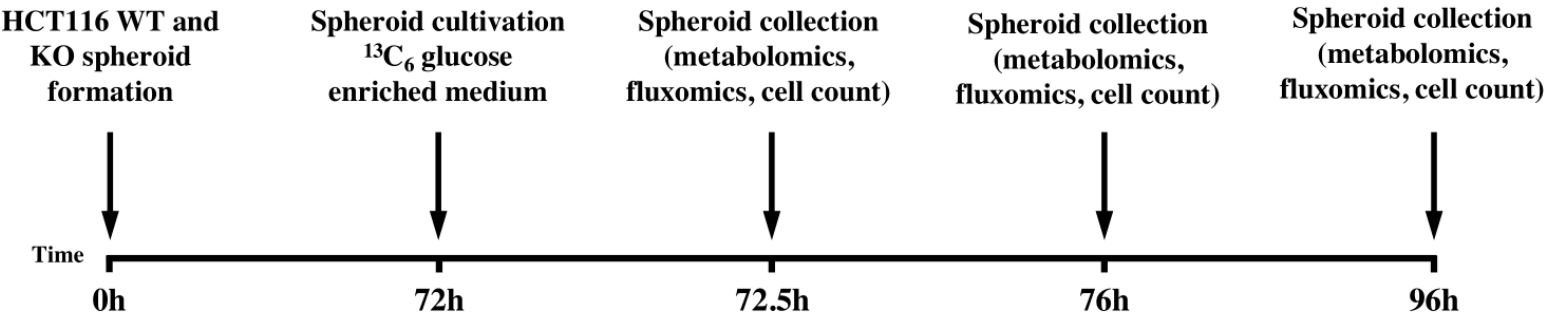
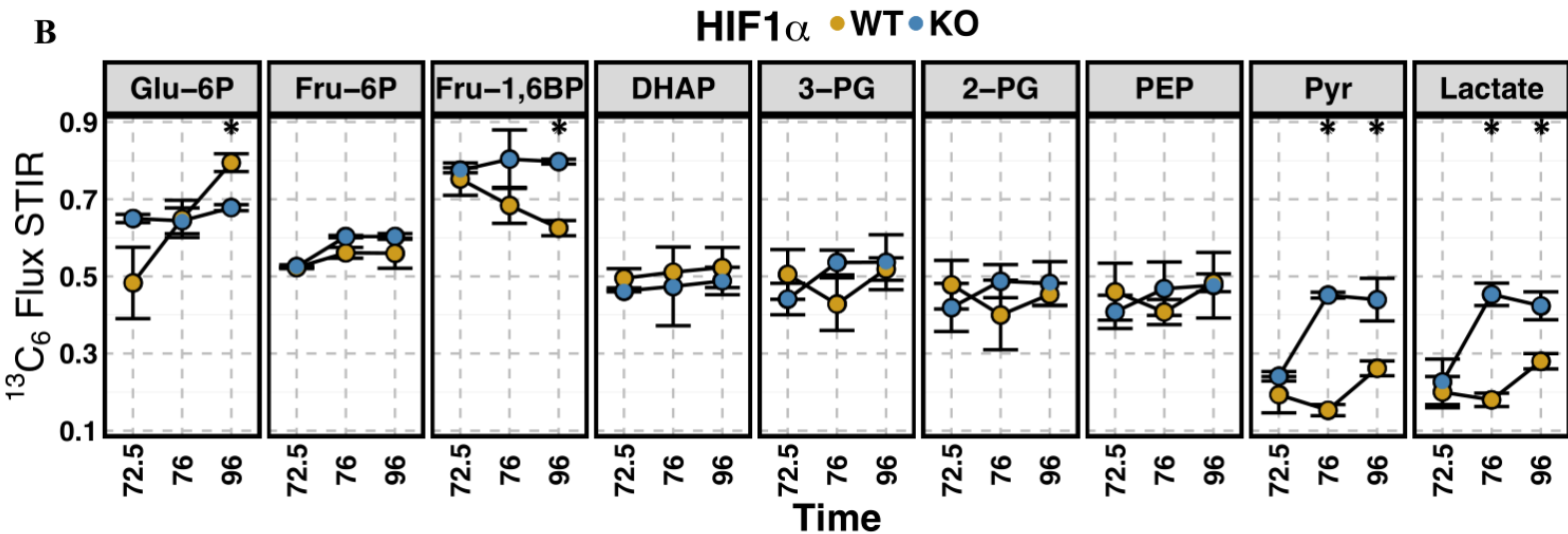


Figure 2

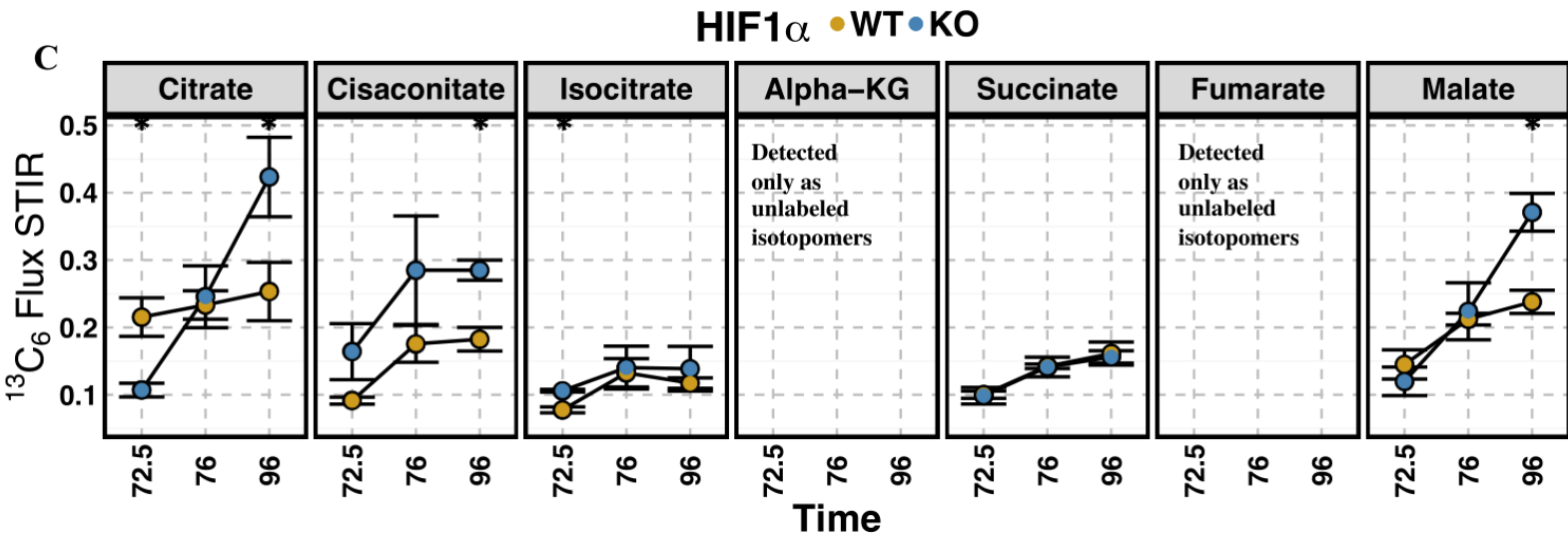
A



B



C



D

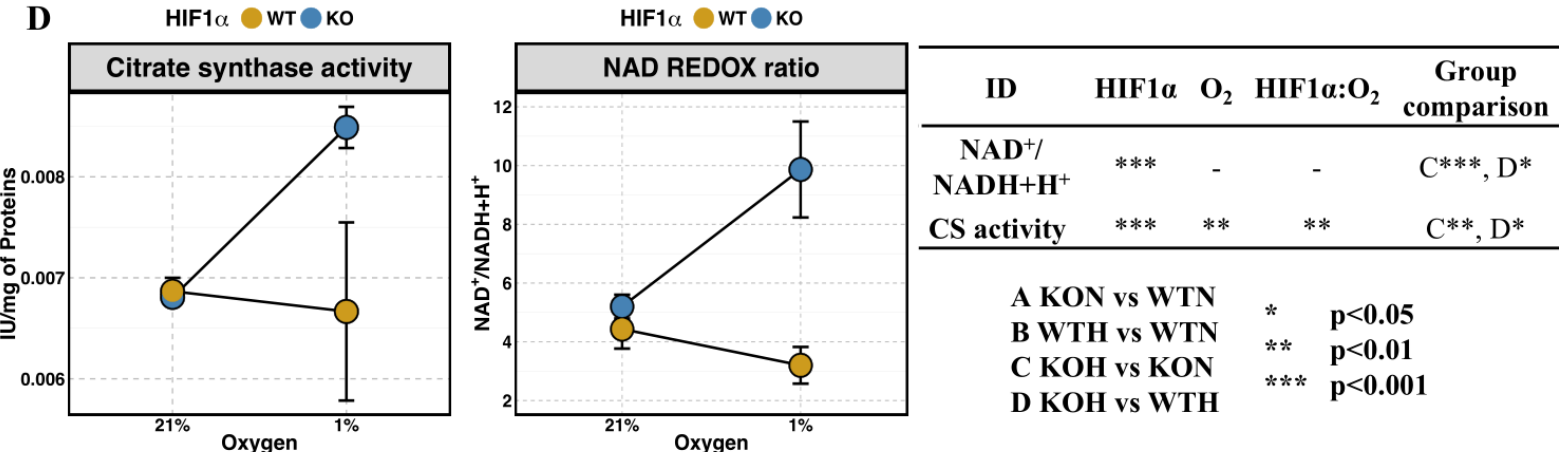


Figure 3

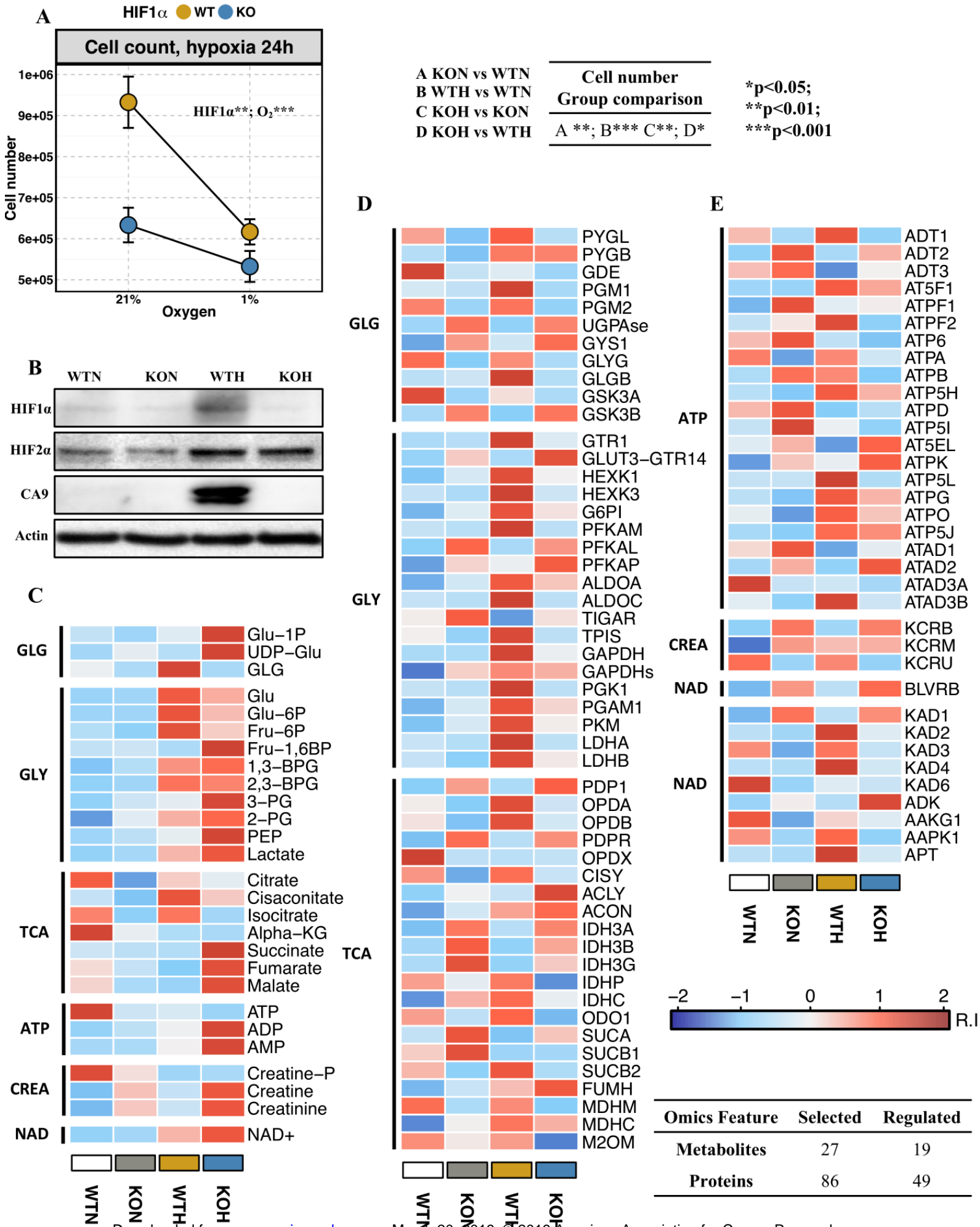


Figure 4

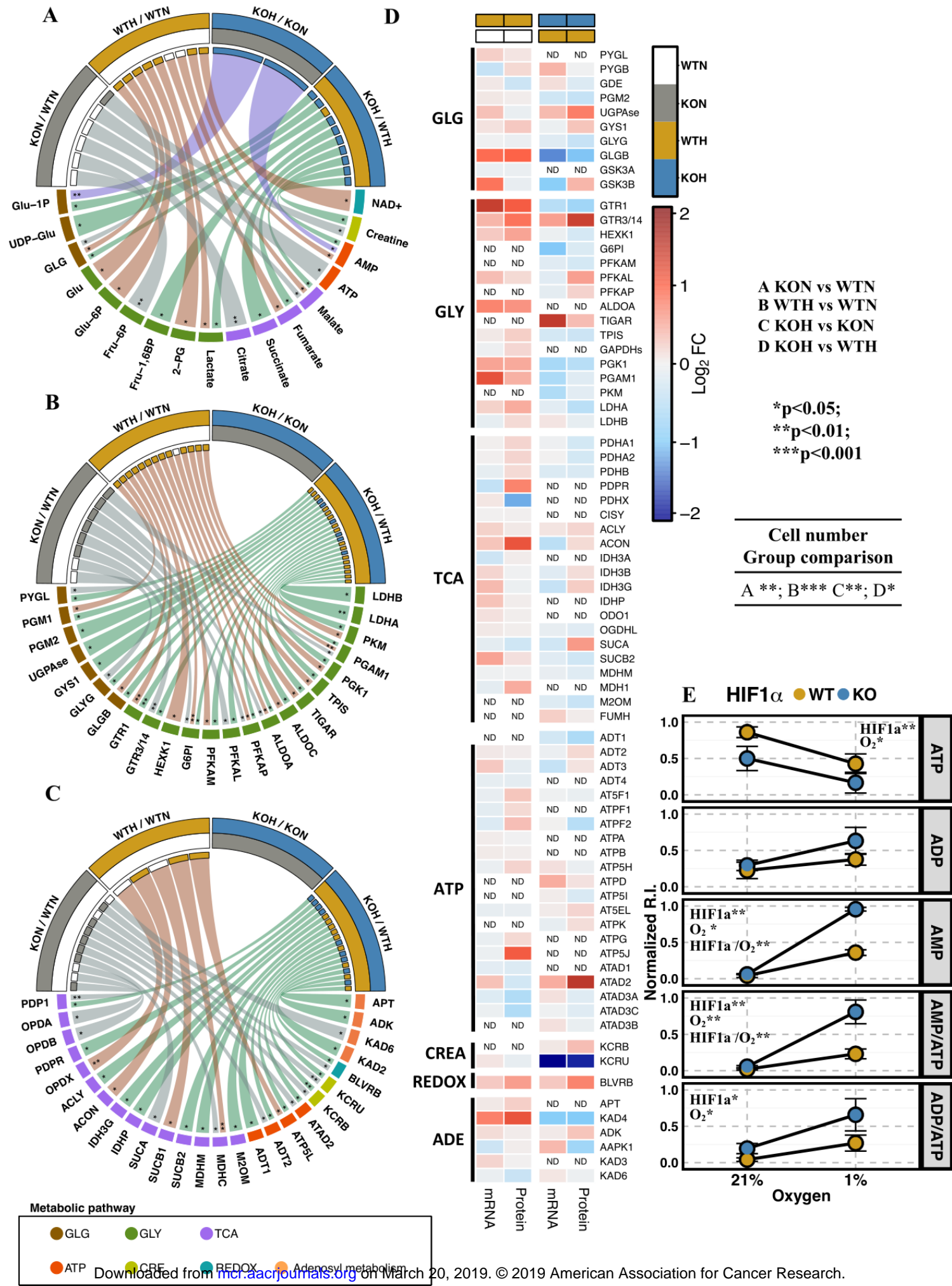


Figure 5

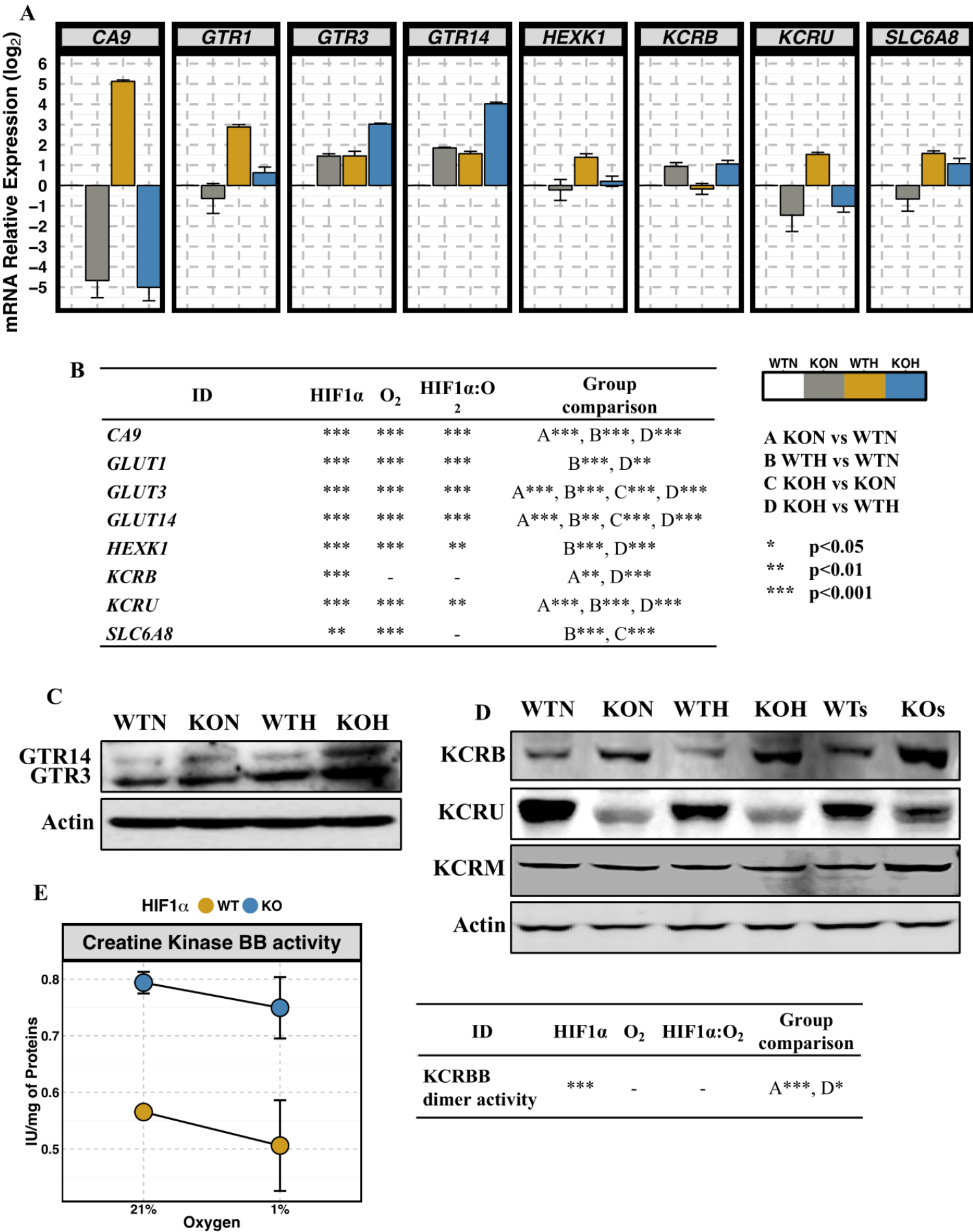


Figure 6

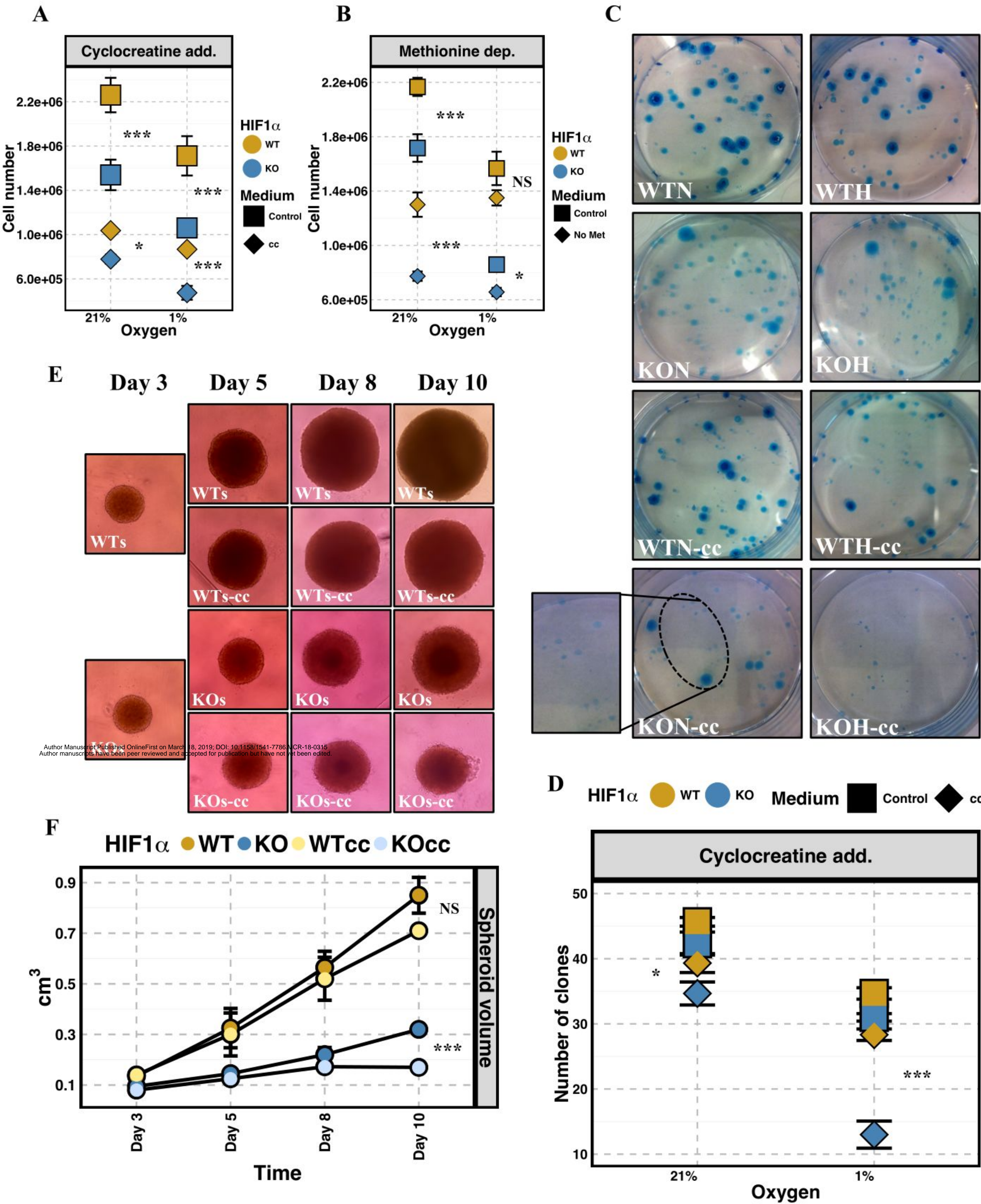
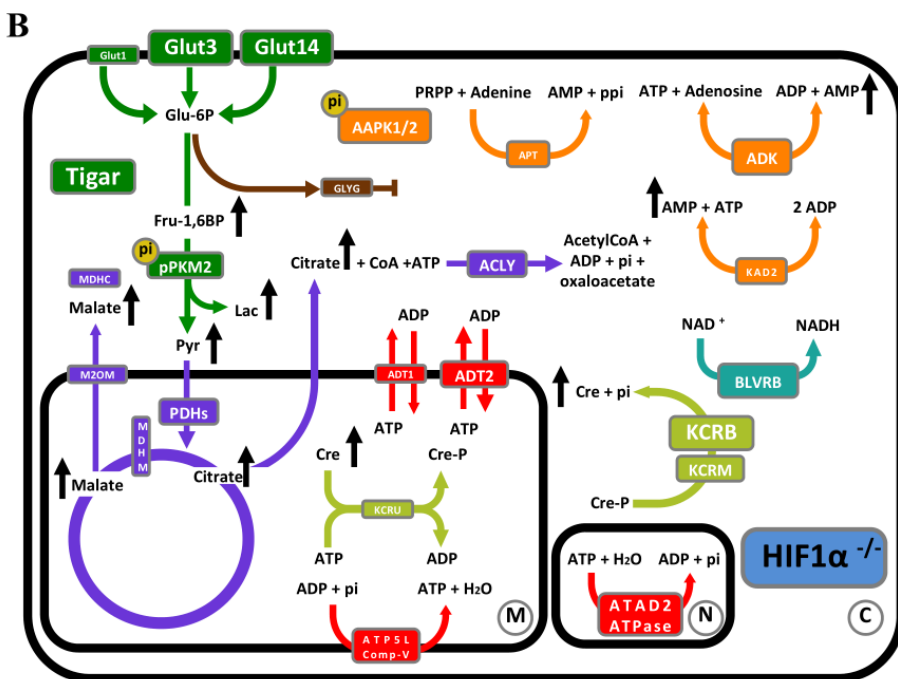
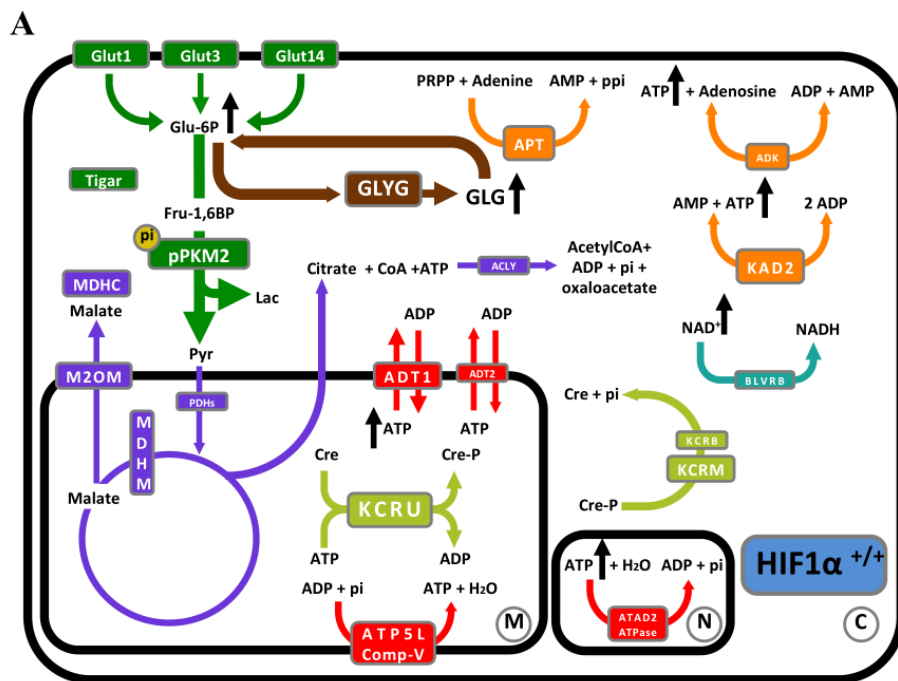


Figure 7



Metabolic pathway



Molecular Cancer Research

Adaptation to HIF1 α deletion in hypoxic cancer cells by upregulation of GLUT14 and creatine metabolism

Alessandro Valli, Matteo Morotti, Christos E Zois, et al.

Mol Cancer Res Published OnlineFirst March 18, 2019.

Updated version	Access the most recent version of this article at: doi: 10.1158/1541-7786.MCR-18-0315
Supplementary Material	Access the most recent supplemental material at: http://mcr.aacrjournals.org/content/suppl/2019/03/16/1541-7786.MCR-18-0315.DC1
Author Manuscript	Author manuscripts have been peer reviewed and accepted for publication but have not yet been edited.

E-mail alerts	Sign up to receive free email-alerts related to this article or journal.
Reprints and Subscriptions	To order reprints of this article or to subscribe to the journal, contact the AACR Publications Department at pubs@aacr.org .
Permissions	To request permission to re-use all or part of this article, use this link http://mcr.aacrjournals.org/content/early/2019/03/16/1541-7786.MCR-18-0315 . Click on "Request Permissions" which will take you to the Copyright Clearance Center's (CCC) Rightslink site.